analytical chemistry

LETTER

pubs.acs.org/ac

Trinitrotoluene Explosive Lights up Ultrahigh Raman Scattering of Nonresonant Molecule on a Top-Closed Silver Nanotube Array

Haibo Zhou,[†,‡] Zhongping Zhang,[*,†,‡] Changlong Jiang,[†] Guijian Guan,[†] Kui Zhang,[†,‡] Qingsong Mei,[†,‡] Renyong Liu,[†] and Suhua Wang[*,†,‡]

[†]Institute of Intelligent Machines, Chinese Academy of Sciences, Hefei, Anhui, 230031, China

[‡]Department of Chemistry, University of Science & Technology of China, Hefei, Anhui, 230026, China

Supporting Information

ABSTRACT: The highest Raman enhancement factors are obtained in a double resonance: molecular electronic resonance and plasmon resonance with a "hot spot" in surface-enhanced Raman scattering (SERS). However, for most molecules of interest the double resonance is not realized with the excitation frequencies normally used in Raman. The latter may limit the practical applications of SERS for trace analysis. Here, we report that Raman-inactive trinitrotoluene (TNT) lights up the ultrahigh Raman scattering of off-resonated *p*-aminobenzenethiol (PABT) through the formation of charge-transfer TNT-PABT complex on the top-closed flexible silver nanotube array. Raman hot spots can spontaneously form in a reversible way by the self-approaching of flexible nanotubes driven through the capillary force of solvent evaporation. Meanwhile, the PABT-TNT-PABT bridges between self-approaching silver nanotubes possibly form by the specific complexing and zwitterion interactions, and the resultant chromophores can absorb the visible light that matches with the incident laser and the localized surface plasmon of a silver nanotube array. The multiple spectral resonances lead to the huge enhancement of Raman signals of PABT molecules due to the presence of ultratrace TNT. The enhancement effect is repeatedly renewable by the reconstruction of molecular bridges and can selectively detect TNT with a limit of 1.5×10^{-17} M. The results in this report provide the simple and supersensitive approach to the detection of TNT explosives and the possibility of building a robust Raman-based assay platform.

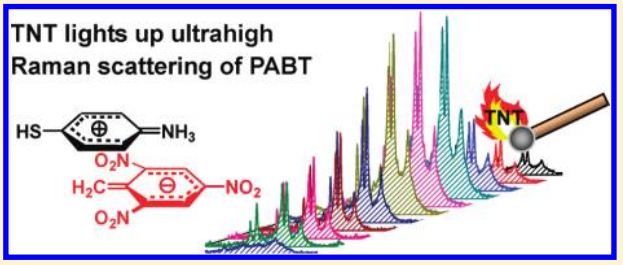

Since the discovery that Raman signals are enhanced at a rough silver electrode,[1−3] surface-enhanced Raman scattering (SERS) has been a subject of interest in research for both the understanding of the enhancement mechanism and the chemosensing purpose. The amplification of scattering signal is generally attributed to the electromagnetic (EM) field near the metal surface.[2−8] Recently, electronically resonated dyes have frequently evidenced the ultrahigh Raman enhancement and the single molecule Raman spectroscopy on the nanoparticle aggregates[9,10] or at the nanostructural junctions ("hot spots")[9−18] that maximize the EM field experienced by a dye molecule. The enhancement factors as large as $10^{11}-10^{14}$ were claimed. These reports further reinforce the belief on the local EM enhancement mechanism[11,12] and have recently stimulated the hottest efforts for the fabrication of various Raman-active substrates such as nanoparticle dimers,[13] nanogaps,[14,15] nanowire/nanorod arrays,[16,17] and periodic 2D nanostructures.[11,18] However, the subnanometer control on the interspace between two nanostructures has to face the problems with a structural reproducibility and low yield. Furthermore, steric hindrance may prevent a molecule into the gaps even if they are precisely prefabricated. In addition, some researchers have also argued that the classical electrodynamic simulation tends to overestimate the role of the local EM field in Raman enhancement.[19−21] Recently, the formation of hot spots by the self-conglutination of nanorods to trap molecules among nanorods may provide a new approach to overcome these difficulties,[17] but the most desirable hot spots for practically chemosensing purpose should be reversible and renewable.

On the other hand, although the local EM strategies provide a new possibility for vibrational spectroscopy of a single molecule, they also give the general impression that only can the resonant dyes such as rhodamine-6G (R6G) and crystal violet exhibit a boost of the Raman intensity enabling the single molecule effect observable. The visible chromophores of resonant dyes may provide 2−3 orders of magnitude of additional enhancement relative to surface enhancement alone.[4−10,22] However, most of the interesting analytes have a much smaller scattering cross section than resonant dyes[23] and as such their Raman signals are extremely weak even if enhanced. Recently, surface-enhanced resonance Raman scattering (SERRS) has been demonstrated as a promising approach to the amplification of Raman signals.[24−27] Bianalyte techniques by adding[24] or modifying a chromophore[25] can enhance the Raman signals of preresonant molecules. The chromophore coupled to the localized surface plasmon of plasmonically active nanostructure led to spectral, resonant, and surface enhancements.[26,27] These imply that the ultrahigh Raman

Received: June 3, 2011
Accepted: August 19, 2011
Published: August 19, 2011

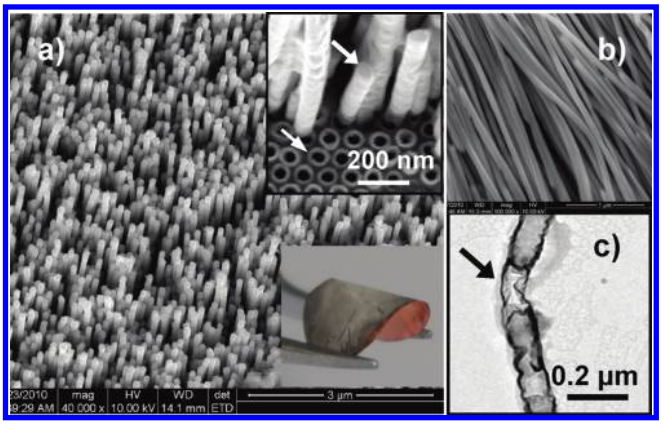

Figure 1. (a) SEM image of a top-closed silver nanotube array (the upper inset shows the cross section of the nanotube array; the bottom inset is the photograph of the nanotube array on a copper substrate). (b) SEM image of the individual nanotubes liberated completely from an alumina template. (c) TEM image of silver nanotubes.

scattering of nonresonant molecules is possible by multiple resonance techniques.

Herein, we report that trinitrotoluene (TNT) explosive lights up the Raman scattering of off-resonated *p*-aminobenzenethiol (PABT) through the rapid formation of a charge-transfer TNT-PABT complexing chromophore on the top-closed flexible silver nanotube array. The main purpose of this current work is threefold: (a) it is shown that Raman hot spots can spontaneously form in a reversible way by the self-approaching of flexible nanotubes driven through the capillary force of solvent evaporation; (b) we present the experimental proofs that the PABT-TNT-PABT chromophore bridge between self-approaching silver nanotubes initiates the ultrahigh Raman scattering of PABT by the spectral resonance with both the incident laser and localized surface plasmon; (c) the Raman response provides an ultrasensitive method for the selective detection of TNT explosive with a limit of 1.5×10^{-17} M. The detection of explosives has been a pressing societal concern.[28−31]

RESULTS AND DISCUSSION

Top-closed silver nanotubes were grown in a highly ordered porous alumina template by electrochemical reduction of $AgNO_3$.[32] A thick layer of metal copper was then deposited on one side of the template (see the Supporting Information for more experimental details). After the removal of the template by dissolving alumina with H_3PO_4, the free-standing silver nanotube array was obtained (Figure 1a). The tubular structure and closed end are clearly revealed by the SEM observation of the cross section (upper inset in Figure 1a), and the large-area nanotube array on copper substrate exhibits a high mechanical strength (bottom inset in Figure 1a). The individual nanotubes are highly uniform in ∼10 μm length, 80 nm diameter (Figure 1b), and 12 nm wall thickness. The thin-walled nanotubes easily bend/deform under electron-ray irradiation (Figure 1c), suggesting a high flexibility for their self-approaching and thus the formation of Raman hot spots.

We first evaluated the SERS effect of the unmodified silver nanotube array. When 1×10^{-14} M R6G ethanol was directly added onto the array, the Raman signals of R6G could clearly be detected and the huge enhancement mainly resulted from the Raman hot spots formed by the self-approaching of flexible silver nanotubes due to the capillary force of solvent evaporation (see Figures S5 and S6 in the Supporting Information). The closed top of nanotubes can prevent analyte solution into the interiors of nanotubes, producing the stronger capillary force and better enhancement effect by the comparison with top-open nanotubes. Meanwhile, the similar observation was also carried out using electronically off-resonated PABT molecules and measured an enhancement factor of $\sim 1 \times 10^8$. On the other hand, the addition of TNT ethanol even at a high concentration of 1×10^{-6} M onto this bare array did not produce any Raman signal of TNT, suggesting non-Raman activeness of TNT (see Figure S7 in the Supporting Information).[33]

The silver nanotube array was further modified with PABT through the formation of Ag−S bonds by immersing the array in very dilute PABT ethanol (1×10^{-9} M). The Raman signals of PABT molecules cannot nearly be detected due to an extremely low number of molecules at this dry array. If a droplet of ultrapure water was added onto the dry nanotube array, there also was not any Raman signal of PABT observed with an increase of observed time (Figure 2a) and the measurement of contact angle revealed a highly hydrophobic feature of the nanotube array (inset microscopic image of Figure 2a). When a droplet of 30 μL of ethanol was added onto the identical nanotube array, however, ethanol completely permeated into the interspaces of the top-closed nanotubes (inset of Figure 2b) and the Raman spectra were recorded at an interval of 17 s. Interestingly, with accompaniment of the evaporation of ethanol, the weak Raman signals of PABT gradually appeared after ∼30 s and achieved the strongest value at ∼85 s (Figure 2b). Subsequently, the signals became weaker and weaker and finally disappeared after the evaporation was completed. These temporally spectral evolutions confirm that the capillary force from the ethanol evaporation drove the self-approach of silver nanotubes to form the hot spots, making the Raman signals of PABT measurable.

When we repeated the above process with only 0.1 pM TNT ethanol, it was surprising that the Raman signals of PABT were violently enhanced (Figure 2c). The strongest signal intensity at 1434 cm^{-1} after ∼100 s is at least ∼4-fold that obtained by the addition of pure ethanol. Similarly, the Raman signals of PABT gradually disappeared with the evaporation of solvent to dryness. When a droplet of ethanol was subsequently added at this dry site, the same evolutions of Raman spectra from a gradual increase to a gradual decrease were again observed, and the identical intensity of the Raman signals at 1434 cm^{-1} was detected after ∼100 s for every cycle (Figure 2d). Repeating the addition of ethanol for 5 cycles did not decrease the Raman intensity of PABT, which fully suggests the renewable ability of PABT Raman signals and the extremely strong interactions between TNT and PABT at this nanotube array. It is assumed that the pure ethanol and 0.1 pM TNT ethanol have the identical evaporation speed and capillary force due to the extremely low TNT concentration. The enhancement of PABT Raman spectra is completely attributed to the contribution of ultratrace TNT.

The mechanism for TNT-induced resonance Raman enhancement of PABT is proposed in Scheme 1. Upon the addition of TNT ethanol onto the top-closed silver nanotube array, the ethanol evaporation drives the self-approach of neighboring flexible nanotubes by capillary force, which will yield a number of Raman hot spots by EM enhancement. Meanwhile, TNT molecules are immediately captured by silver nanotubes through the formation of the TNT-PABT complex. Followed by the self-approach of the nanotubes, the PABT-TNT-PABT molecular

dx.doi.org/10.1021/ac201407z |*Anal. Chem.* 2011, 83, 6913–6917

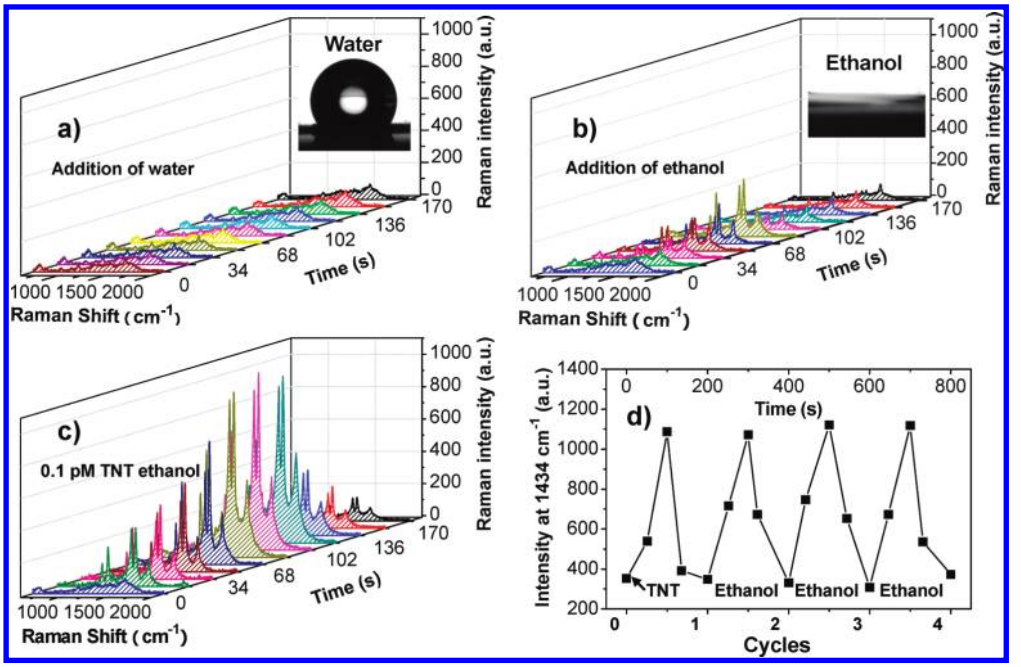

Figure 2. The time-resolved Raman spectra of PABT at the interval of 17 s after dropping 30 μL of (a) water, (b) ethanol, and (c) 0.1 pM TNT ethanol on the PABT-modified nanotube array. The insets in parts a and b are the photographs of water and ethanol droplets at the substrate, respectively. (d) Cyclic detection of PABT Raman intensity at 1434 cm^{-1} after adding 30 μL of 0.1 pM TNT ethanol, which was followed by adding 30 μL of pure ethanol after the dryness of TNT ethanol. All Raman spectra were recorded with a 532 nm laser with 1 mW power and 50× objective (1 μm^2 spot).

Scheme 1. Mechanism for TNT-Induced Resonance Raman Enhancement of PABT on the Top-Closed Silver Nanotube Array[a]

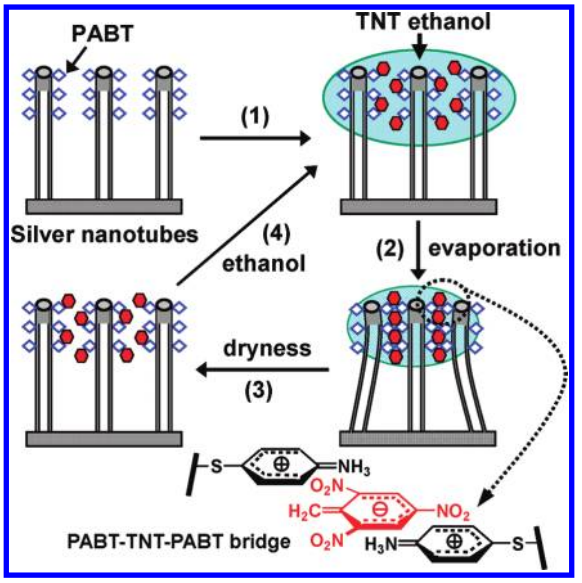

[a] Self-approach of the nanotubes driven by the capillary force of solvent evaporation and the formation of the charge transfer PABT-TNT-PABT complexing bridges between nanotubes.

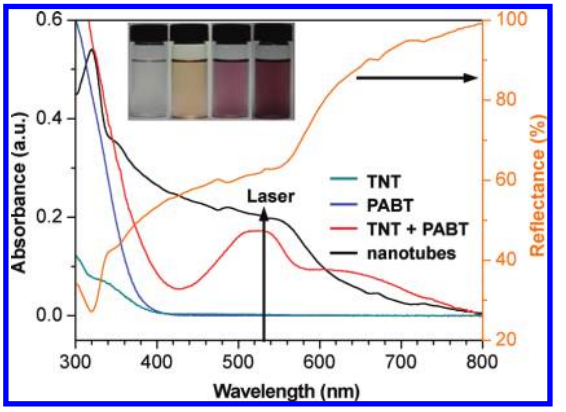

Figure 3. UV−vis absorption spectra of TNT, PABT, TNT-PABT complex, and top-closed silver nanotube array. The inset images show the colors with the addition of 0, 40, 120, and 200 μL of 0.01 M PABT into 4 mL of 0.1 mM TNT solution, respectively. The UV−vis spectra in solution were obtained using ethanol as the solvent at room temperature with a path-length of 1 cm. The UV−vis spectrum of the top-closed Ag nanotube arrays was transformed with an integral sphere detector unit by a reflectance spectrum.

bridges between nanotubes are temporally constructed. Our previous research[28,29] has confirmed that the TNT molecule is deprotonated at the methyl group by the electron-rich amine, leading to the formation of the charge-transfer Meisenheimer complex. The negative charge on the TNT anion is distributed throughout the aromatic ring through the resonance stabilization by three electron-withdrawing nitro groups. Here, the formation of the TNT-PABT complex can be clearly evidenced by a new absorption at the 529 nm (the red line in Figure 3) and a color mutation from colorless to deep purple (the inset image of Figure 3). The formation of the molecular bridge is the result of (1) the countercharged interaction between TNT(−) and PABT(+); (2) the self-approach of nanotubes by capillary force; (3) the immobilization of PABT on the silver nanotubes. The alternate arrangement of countercharged ions occurs between self-approaching nanotubes, in which TNT(−) ions are located between PABT(+) layers in an overview. Therefore, the

dx.doi.org/10.1021/ac201407z |*Anal. Chem.* 2011, 83, 6913–6917

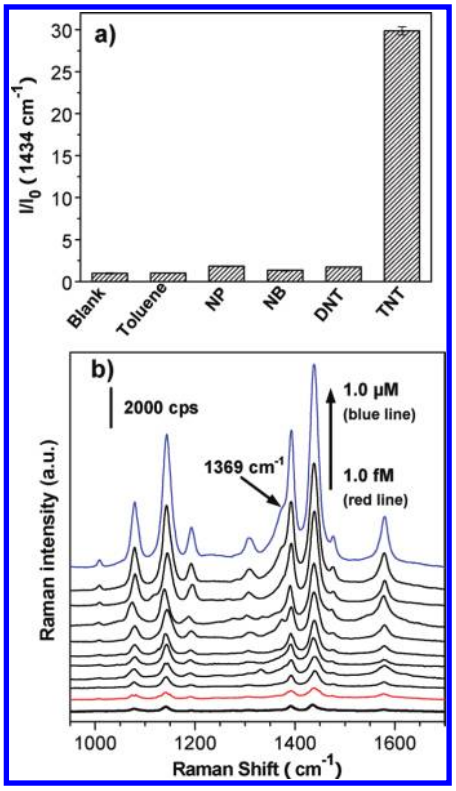

Figure 4. (a) Selectivity of PABT Raman enhancement (I/I_0) to structure-like molecules (1.0 μM in ethanol): toluene, nitrophenol (NP), nitrobenzene (NB), dinitrotoluene (DNT), and TNT (I and I_0 represent the Raman intensity at 1434 cm^{-1} in the presence and absence of analytes, respectively). (b) Evolution of Raman spectra of PABT with the increase of TNT concentrations from 1.0 fM to 1.0 μM by a factor of 10 (the bottom dark line represents the addition of the blank ethanol).

structures can be regarded as the molecular bridge in the current work, which may further enhance the Raman spectrum of PABT.[34]

When the 532 nm laser is used to record the Raman spectrum, the complexing chromophore absorbs the light and brings about the electronic resonance of the molecular bridge and thus the enhancement of the PABT Raman signals. Meanwhile, the spectral overlap between the chromophore absorption and the surface plasmon of silver nanotubes (500−600 nm, black line in Figure 3) may lead to the surface resonance enhancement.[26,27] Therefore, the Raman enhancement of PABT results from the multiple spectral resonances. If the liquid droplet evaporates to dryness, the nanotubes will recover to the free-standing state, the molecular bridges and Raman spots are deconstructed, and as a result, the Raman signals of PABT gradually disappear. According to the mechanism, we can also imagine that Raman signals of PABT are repeatedly renewable when a droplet of ethanol is added at this above dry site, as evidenced in Figure 2d.

At this time of the self-approach of the nanotubes, three possible Raman effects will occur. First, the Raman hot spots are formed at intimate interspaces between the self-approaching nanotubes. The relation between the Raman intensity, I, and the local EM strength, E, is usually approximated as $I \propto |E|^4$.[26,27,35] If other effects are not considered, the formation of PABT-TNT-PABT will increase the distance of two self-approaching nanotubes from D_0 to D_1, and the relation between E and interspace distance, D, is described as $E \propto (D_0/D_1)^5$,[36] which may decrease the enhancement effect of hot spots. Second, the extended conjugation system of PABT-TNT-PABT absorbs the incident laser of 532 nm, bringing the PABT into a resonant state to thus enhance the Raman scattering of PABT. Third, considering the molecular bridge as an integrity, the chromophore located between the nanotubes is wavelength matched with the surface plasmon resonance of the silver nanotubes, generating a surface resonance-enhanced spectrum.[26,27] It should be noted that when a 780 nm laser was used, there was not PABT Raman signals observed for all measurements. These analyses confirm that the enormous Raman enhancement mainly originates from the resonances of the molecular bridge with both incident laser and surface plasmon, with the aid of Raman hot spots formed by the self-approach of the nanotubes.

To better understand the enhancement mechanism, we have compared the enhancement effects by the addition of other structural-like analytes (1 μM in ethanol): toluene, nitrophenol (NP), nitrobenzene (NB), and dinitrotoluene (DNT) (Figure 4a). Toluene did not cause any change of Raman intensity that was identical to the blank ethanol. The extremely slight enhancement was observed by the addition of NP, NB, and DNT. Although DNT has the most similar structure to TNT and exhibits the weak interaction with amines,[28−31] the UV−vis spectrum does not show any visible absorption when DNT is mixed with PABT in solution, suggesting that DNT cannot likely form the effective charge-transfer complexing chromophore with PABT (see Figure S8 in the Supporting Information).

Moreover, other Raman signal molecules with thiol groups, including methoxybenzenethiol, mercaptotoluene, and naphthalenethiol, were also modified at a much higher concentration (1×10^{-4} M) on the silver nanotube array. Even if 1 μM TNT ethanol was dropped on these modified arrays, there were only the extremely weak Raman signals of these molecules detected (see Figure S10 in the Supporting Information). The high spectral selectivity of PABT to TNT again suggests that the complexing chromophores play a crucial role in enhancing the Raman scattering of PABT.

The strategy also provides an ultrasensitive and selective method for the detection of TNT explosive by the Raman enhancement of PABT modified on the silver nanotube array. On the basis of the above results, the best measuring conditions for the detection of TNT were thus set at the volume of a 30 μL analyte droplet, data recorded at ~100 s after the addition of the liquid droplet, and the use of a 1 mW and 1 μm^2 laser beam. As shown in Figure 4b, the Raman intensity of PABT obviously increases with TNT concentrations from 1.0 fM to 1.0 μM and exhibits a correlation coefficient $R = 0.9945$ at the range of 1.0 fM to 10 pM and a corresponding standard deviation SD = 1.4712. Even in the case of 1.0 fM TNT, the Raman signal of PABT is 1.7-fold stronger than that by the addition of blank ethanol, and thus a detection limit of 1.5×10^{-17} M TNT is reached (see Figure S11 in the Supporting Information).

In addition, it should be noted that the Raman signals of TNT may simultaneously be detected by the resonance enhancement technology upon the formation of the TNT-PABT chromophore complex. At the PABT-modified silver nanotube array, the weak Raman signals of TNT were monitored at a relatively high concentration. The strongest peak of TNT at 1369 cm^{-1} became the left shoulder of strong PABT Raman peaks at 1390 cm^{-1}, as indicated with an arrow in Figure 4b. In most cases, however, the weak peaks of the Raman spectra of the TNT molecule were usually embedded in the background of the extremely strong Raman spectrum of PABT.

In summary, the self-approach of the nanotubes driven by the capillary force of solvent evaporation is an extremely simple and efficient strategy for the spontaneous formation of Raman hot spots and is highly reversible for the reproduction of hot spots and the repeating usage. Importantly, it has been demonstrated that creating the chromophores resonate with the incident laser and localized surface plasmon can initiate the Raman scattering of nonresonant molecules by a huge enhancement factor that is comparable to that of electronically resonated dyes. The combination of a resonance enhancement mechanism with the nanotube array provides the best possibility of building a robust SERS-based assay platform. Finally, the sensitivity, selectivity, and simplicity of the strategy for the detection and identification of TNT explosive exceed the currently existing methods. To extend the method and mechanism in this report to supramolecular chemistry may allow for ultrasensitive probing of other organic and biological species.

■ ASSOCIATED CONTENT

Supporting Information. Structures of Raman-signal molecules and analytes, UV absorbance spectra, and Raman spectra. This material is available free of charge via the Internet at http://pubs.acs.org.

■ AUTHOR INFORMATION

Corresponding Author
*E-mail: zpzhang@iim.ac.cn (Z.Z); shwang@iim.ac.cn (S.W.).

■ ACKNOWLEDGMENT

This work was supported by the Natural Science Foundation of China (Grants 20925518, 20875090, 61071055, and 21077108), the China-Singapore Joint Research Project (Grant 2009DFA51810), and the Innovation Project of Chinese Academy of Sciences (Grants KSCX2-YW-G-058 and KJCX2-YW-H29).

■ REFERENCES

(1) Fleischmann, M.; Hendra, P. J.; McQuillan, A. J. *Chem. Phys. Lett.* **1974**, *26*, 163–166.
(2) Jeanmaire, D. L.; Van Duyne, R. P. *J. Electroanal. Chem.* **1977**, *84*, 1–20.
(3) Albrecht, M. G.; Creighton, J. A. *J. Am. Chem. Soc.* **1977**, *99*, 5215–5217.
(4) Schatz, G. C. *Acc. Chem. Res.* **1984**, *17*, 370–376.
(5) Moskovits, M. *Rev. Mod. Phys.* **1985**, *57*, 783–826.
(6) Surface Enhanced Raman Scattering, Physics and Applications. In *Topics in Applied Physics*; Kneipp, K., Moskovits, M., Kneipp, H., Eds.; Springer: Berlin, Germany, 2006; Vol. 103.
(7) Otto, A.; Mrozek, I.; Grabhorn, H.; Akemann, W. *J. Phys.: Condens. Matter* **1992**, *4*, 1143–1212.
(8) Willets, K. A.; Van Duyne, R. P. *Annu. Rev. Phys. Chem.* **2007**, *58*, 267–297.
(9) Nie, S. M.; Emory, S. R. *Science* **1997**, *275*, 1102–1106.
(10) Kneipp, K.; Wang, Y.; Kneipp, H.; Perelman, L. T.; Itzkan, I.; Dasari, R. R.; Feld, M. S. *Phys. Rev. Lett.* **1997**, *78*, 1667–1670.
(11) Fang, Y.; Seong, N. H.; Dlott, D. D. *Science* **2008**, *321*, 388–392.
(12) Pieczonka, N. P. W.; Aroca, R. F. *Chem. Soc. Rev.* **2008**, *37*, 946–954.
(13) Lim, D. K.; Jeon, K. S.; Kim, H. M.; Nam, J. M.; Suh, Y. D. *Nat. Mater.* **2010**, *9*, 60–67.
(14) Sawai, Y.; Takimoto, B.; Nabika, H.; Ajito, K.; Murakoshi, K. *J. Am. Chem. Soc.* **2007**, *129*, 1658–1662.
(15) Li, S. Z.; Pedano, M. L.; Chang, S. H.; Mirkin, C. A.; Schatz, G. C. *Nano Lett.* **2010**, *5*, 1722–1727.
(16) Lee, S. J.; Morrill, A. R.; Moskovits, M. *J. Am. Chem. Soc.* **2006**, *128*, 2200–2201.
(17) Hu, M.; Ou, F. S.; Wu, W.; Naumov, I.; Li, X. M.; Bratkovsky, A. M.; Williams, R. S.; Li, Z. Y. *J. Am. Chem. Soc.* **2010**, *132*, 12820–12822.
(18) Stuart, D. A.; Yonzon, C. R.; Zhang, X. Y.; Lyandres, O.; Shah, N. C.; Glucksberg, M. R.; Walsh, J. T.; Van Duyne, R. P. *Anal. Chem.* **2005**, *77*, 4013–4019.
(19) Zuloaga, J.; Prodan, E.; Nordlander, P. *Nano Lett.* **2009**, *9*, 887–891.
(20) Blackie, E. J.; Le Ru, E. C.; Etchegoin, P. G. *J. Am. Chem. Soc.* **2009**, *131*, 14466–14472.
(21) Park, W. H.; Kim, Z. H. *Nano Lett.* **2010**, *10*, 4040–4048.
(22) Doering, W. E.; Nie, S. M. *Anal. Chem.* **2003**, *75*, 6171–6176.
(23) Maher, R. C.; Galloway, C. M.; Le Ru, E. C.; Cohen, L. F.; Etchegoin, P. G. *Chem. Soc. Rev.* **2008**, *37*, 965–979.
(24) Le Ru, E. C.; Meyer, M.; Etchegoin, P. G. *J. Phys. Chem. B* **2006**, *110*, 1944–1948.
(25) Pieczonka, N. P. W.; Moula, G.; Aroca, R. F. *Langmuir* **2009**, *25*, 11261–11264.
(26) Witlicki, E. H.; Andersen, S. S.; Hansen, S. W.; Jeppesen, J. O.; Wong, E. W.; Jensen, L.; Flood, A. H. *J. Am. Chem. Soc.* **2010**, *132*, 6099–6107.
(27) Hirakawa, A. Y.; Tsuboi, M. *Science* **1975**, *188*, 359–361.
(28) Xie, C. G.; Zhang, Z. P.; Wang, D. P.; Guan, G. J.; Gao, D. M.; Liu, J. H. *Anal. Chem.* **2006**, *78*, 8339–8346.
(29) Gao, D. M.; Zhang, Z. P.; Wu, M. H.; Xie, C. G.; Guan, G. J.; Wang, D. P. *J. Am. Chem. Soc.* **2007**, *129*, 7859–7866.
(30) Dasary, S. S. R.; Singh, A. K.; Senapati, D.; Yu, H. T.; Ray, P. C. *J. Am. Chem. Soc.* **2009**, *131*, 13806–13812.
(31) Riskin, M.; Tel-Vered, R.; Bourenko, T.; Granot, E.; Willner, I. *J. Am. Chem. Soc.* **2008**, *130*, 9726–9733.
(32) Yang, D. C.; Meng, G. W.; Zhang, S. Y.; Hao, Y. F.; An, X. H.; Wei, Q.; Ye, M.; Zhang, L. D. *Chem. Commun.* **2007**, *17*, 1733–1735.
(33) McHugh, C. J.; Keir, R.; Graham, D.; Smith, W. E. *Chem. Commun.* **2002**, *6*, 580–581.
(34) Zhou, Q.; Li, X. W.; Fan, Q.; Zhang, X. X.; Zheng, J. W. *Angew. Chem., Int. Ed.* **2006**, *45*, 3970–3973.
(35) Campion, A.; Kambhampati, P. *Chem. Soc. Rev.* **1998**, *27*, 241–250.
(36) Kim, N. H.; Lee, S. J.; Moskovits, M. *Nano Lett.* **2010**, *10*, 4181–4185.